Tunable Left-Handed Characteristics of Ferrite Rectangular Waveguide Periodically Loaded With Complementary Split-Ring Resonators

J. Ghalibafan[1], N. Komjani[1], and B. Rejaei[2]

[1]Antenna and Microwave Laboratory, Electrical Engineering Department, Iran University of Science and Technology, Tehran 1684613114, Iran

[2]Electrical Engineering Department, Sharif University of Technology, Tehran 1136511155, Iran

We propose, for the first time, a tunable left-handed (LH) waveguide consisting of an array of complementary split-ring resonators built on the broad wall of a rectangular waveguide filled with ferrite material. The left-handed behavior is caused by the negative permittivity of the complementary split-ring resonators together with the negative permeability of the transversely magnetized ferrite. The electromagnetic behavior of this structure is studied by means of an equivalent circuit model. From this model, the dispersion relation of the guide is derived and validated numerically by the finite element method. It is shown that this structure has a left-handed frequency band that can be tuned by changing the dc bias magnetic field applied to the ferrite. Compared to previous works, the fabrication requirements on this structure are not critical, which enhances its potential applicability.

***Index Terms*—Complementary split-ring resonator (CSRR), left-handed media, magnetized ferrite, tunable metamaterial.**

I. Introduction

OVER the last decade, left-handed metamaterials (LHMs) with simultaneous negative permittivity and permeability have attracted considerable attention in optics, physics, and microwave engineering. Such materials do not exist in nature, but are realized by artificial means. They often consist of periodic arrays of metallic particles effectively behaving as homogeneous media like, for example, a regular array of split-ring resonators (SRRs) between the metal thin wires [1]. Furthermore, the left-handed behavior can be realized in planar structures, such as a transmission line periodically loaded with series capacitors and shunt inductors [2]. Most metamaterials, however, suffer from a narrow frequency band of operation that has motivated the study of electrically tunable designs. For instance, application of microelectromechanical switches (MEMS) [3] or microwave varactor diodes and thin film capacitors [4] has been proposed to realize frequency-tunable metamaterials by controlling the resonance properties of the SRR.

The negative effective permeability of ferrite materials at microwave frequencies and its dependence on the applied bias field make these media a prime candidate for implementation of tunable LHMs. For example, Dewar has proposed an LHM by implementing an array of metallic wires inside a ferrite substrate [5]. Several works have been reported by Caloz [6], [7] using uniform ferrite-loaded open waveguide structure with composite right/left-handed (CRLH) response. Left-handed transmission lines have also been realized by using a ferrite substrate in a coplanar waveguide (CPW) [8], [9] or microstrip line [10], [11].

In this paper, we present a novel, tunable left-handed waveguide that consists of a ferrite-filled rectangular waveguide upon whose broad wall an array of complementary split-ring resonators (CSRRs) is etched. The idea here is to realize left-handed properties by combining the negative effective permittivity of the CSRR array with the negative effective permeability of the ferrite. This structure is fully planar (i.e., without lumped elements or vias) and can be easily fabricated by using standard etching techniques.

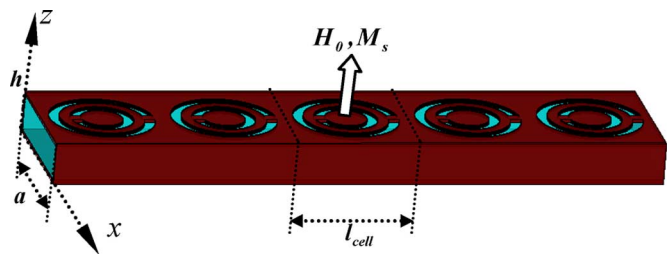

Fig. 1. Geometry of the proposed transversely magnetized ferrite rectangular waveguide periodically loaded with CSRRs. The number of cells $N = 5$.

In Section II, we present an equivalent-circuit model for the CSRR-loaded ferrite-filled waveguide. This model will then be used to derive the analytical dispersion relation that is shown to exhibit left-handed characteristics. In Section III, to verify the theoretical results, the proposed left-handed structure is simulated by commercial software based on finite element method (FEM). Finally, the tunability of the proposed structure versus the magnetic bias is studied.

II. Theory

A. Transversely Magnetized Ferrite-Filled Rectangular Waveguide

Fig. 1 shows the structure proposed in which CSRRs are etched on the upper wall of a ferrite-filled rectangular waveguide. The guide is subject to a bias magnetic field H_0 that is applied perpendicularly to the CSRR plane (along the z-direction). To investigate this system, we first review the properties of the waveguide in the absence of the CSRRs. The primary propagating mode of a rectangular waveguide, fully filled with a transversely magnetized ferrite material is the TE_{10} mode where

Manuscript received October 17, 2012; revised December 03, 2012; accepted January 31, 2013. Date of publication February 06, 2013; date of current version July 23, 2013. Corresponding author: J. Ghalibafan (e-mail: jghalibafan@ee.iust.ac.ir).

Color versions of one or more of the figures in this paper are available online at http://ieeexplore.ieee.org.

Digital Object Identifier 10.1109/TMAG.2013.2245336

the modal electric and magnetic fields are respectively given by [12], [13]

$$\boldsymbol{E} = A_{10}\sin\left(\frac{\pi x}{a}\right)e^{-j\beta_{10}y}\hat{\boldsymbol{z}} \tag{1a}$$

$$\boldsymbol{H} = \frac{A_{10}}{\omega\mu_0\mu_\perp}\left[\beta_{10}\sin\left(\frac{\pi x}{a}\right) - \frac{\pi}{a}\frac{\mu_a}{\mu}\cos\left(\frac{\pi x}{a}\right)\right]e^{-j\beta_{10}y}\hat{\boldsymbol{x}} + \frac{jA_{10}}{\omega\mu_0\mu_\perp}\left[\beta_{10}\frac{\mu_a}{\mu}\sin\left(\frac{\pi x}{a}\right) - \frac{\pi}{a}\cos\left(\frac{\pi x}{a}\right)\right]e^{-j\beta_{10}y}\hat{\boldsymbol{y}}. \tag{1b}$$

Here, a is the width of the guide, μ_0 is the permeability of vacuum, and

$$\mu = 1 + \frac{\omega_H\omega_M}{\omega_H^2 - \omega^2}$$
$$\mu_a = \frac{\omega_M\omega}{\omega_H^2 - \omega^2} \tag{1c}$$

denote the diagonal, respectively, off-diagonal elements of the permeability tensor of the ferrite where

$$\omega_H = \gamma H_0 + j\alpha\omega \quad \omega_M = \gamma M_{\rm s} \tag{1d}$$

with $M_{\rm s}$ the saturation magnetization of the ferrite, γ the gyromagnetic ratio, and α the Gilbert damping constant that accounts for the magnetic precession loss. Moreover

$$\mu_\perp = \mu - \frac{\mu_a^2}{\mu} = \frac{(\omega_H + \omega_M)^2 - \omega^2}{\omega_\perp^2 - \omega^2} \tag{1e}$$

where

$$\omega_\perp = \sqrt{\omega_H(\omega_H + \omega_M)}. \tag{1f}$$

Note that the $\rm TE_{10}$ field components do not change in the vertical (z-direction) and propagate along the guide (y-direction) with the constant [13]

$$\beta_{10} = \sqrt{\omega^2\varepsilon_0\varepsilon\mu_0\mu_\perp - \frac{\pi^2}{a^2}} \tag{2}$$

where ε_0 and ε are the permittivity of vacuum and the relative permittivity of ferrite material, respectively.

The dispersion (2) is identical to that of an ordinary waveguide, except for the fact that the effective permeability $\mu_\perp$ is itself a function of frequency ω. In the frequency range $\omega_\perp < \omega < \omega_H + \omega_M$, where the real part of $\mu_\perp$ becomes negative, no propagation takes place, regardless of the waveguide width. This is the frequency range of interest for our purpose.

B. Equivalent Circuit Model of a Ferrite-Based CSRR

The CSRR-loaded transmission lines and waveguides have been analyzed in various works [14], [15]. The results obtained show the CSRR to behave as a resonator that can be excited by an axial electric field induced by the line. Fig. 2 shows the corresponding equivalent circuit model where C_c and L_c comprise the resonator and the series capacitance C models the coupling between the host line and CSRR [14]. The resulting overall impedance is given by

$$Z_p = \frac{1 - \frac{\omega^2}{\omega_s^2}}{j\omega C\left(1 - \frac{\omega^2}{\omega_0^2}\right)} \tag{3}$$

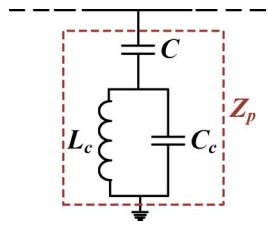

Fig. 2. Equivalent circuit model for the basic cell of the CSRR loaded transmission line.

where $\omega_0 = (L_cC_c)^{-1/2}$ is the resonance frequency of an uncoupled CSRR, and $\omega_s = (L_cC_c + L_cC)^{-1/2}$. Equation (3) indicates the presence of a frequency range $\omega_s < \omega < \omega_0$ where Z_p is inductive. In case of a transmission line periodically loaded with CSRRs, these inductive shunt elements may lead to a negative per-unit-length capacitance, thus negative effective dielectric constant [15]. This point will be addressed later in the context of the ferrite-filled waveguide.

For conventional CSRRs, attempts to directly estimate the circuit parameters of Fig. 2, e.g., by viewing the CSRR as a ring-shaped coplanar waveguide line [14], have produced less than satisfactory outcomes. Numerical extraction techniques, which are based on comparison between full-wave electromagnetic and electrical simulations, appear more reliable [16]. Here, the simulations are carried out for a CSRR coupled to a parallel plate structure, with a dielectric filling of the same permittivity and thickness as that of the waveguide. However, the numerical extraction technique does not seem to work on a ferrite with negative permeability $\mu_\perp$. This is because the propagating modes are non-TEM. Moreover, the negative permeability of the host line complicates the extraction process.

To overcome these drawbacks, we take the capacitors in Fig. 2 to be independent of the magnetic properties of the ferrite material beneath the CSRR. This assumption is motivated by the electrostatic capacitance calculations in the CSRR literature, which are justified if the CSRR dimensions are small compared to the wavelength. Within this method, C_c, C are independent of the magnetic properties of the environment. However, the inductance in Fig. 2 will obviously depend on the permeability of the underlying substrate material.

Therefore, C_c, C will be extracted by considering a CSRR on a dielectric substrate with the same permittivity as the ferrite material. Since the dominant mode in the host parallel plate system is now TEM, this extraction is not troublesome, as shown in Fig. 3. In order to estimate L_c, a second approximation is made where the underlying ferrite substrate is assumed to be infinitely thick. As shown in the Appendix, currents flowing on conductors comprising the CSRR will then experience an effective (relative) permeability

$$\mu_{\rm eff} = \frac{2\sqrt{\mu}}{1 + \sqrt{\mu}}. \tag{4}$$

Therefore, for the calculation of L_c, the value found on a dielectric substrate will be multiplied by (4).

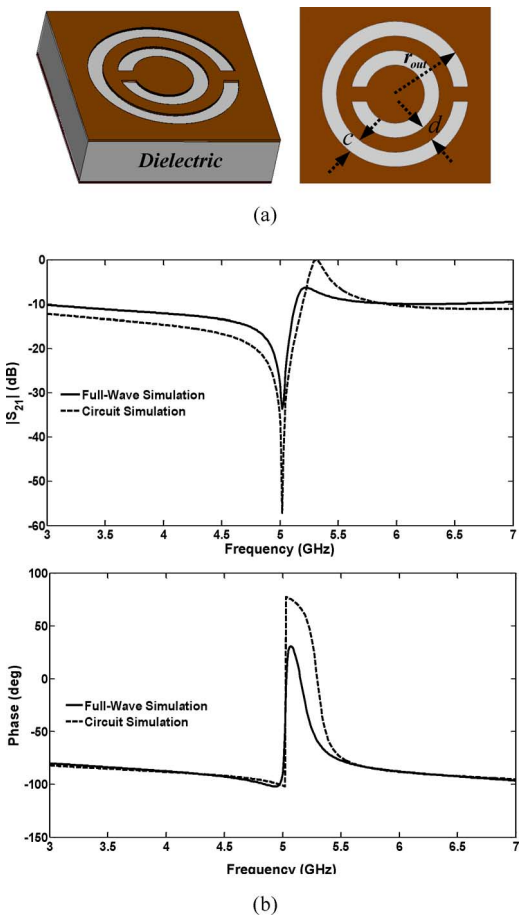

Fig. 3. (a) Geometry of the unit cell of CSRR loaded dielectric parallel-plate waveguide. (b) Transmission and phase characteristics for the unit cell of CSRR loaded dielectric parallel-plate waveguide. The dielectric has thickness $h = 0.5$ mm and dielectric constant $\varepsilon_r = 15.3$. CSRR dimensions are $r_{\text{out}} = 1.5$ mm and $d = c = 0.3$ mm. Extracted parameters of equivalent circuit are $C_c = 0.54$ pF, $C = 1.54$ pF, $L_c = 0.48$ nH.

C. Dispersion Relation of a CSRR-Loaded Ferrite-Filled Rectangular Waveguide

Fig. 4(a) shows a unit cell of the structure of Fig. 1 that is modeled by the equivalent circuit of the CSRR sandwiched between two waveguide sections each of length $l_{\text{cell}}/2$ [see Fig. 4(b)]. The ferrite-filled rectangular waveguide sections are characterized by the propagation constant given in (2) and a nominal characteristic impedance defined by the relation between the complex power transmitted in the y-direction and the current on the waveguide [17]

$$Z_{10} = \frac{2P}{|I|^2} = \frac{\int_0^h \int_0^a E_z \cdot H_x^* dx dz}{\left|\int_0^a H_x dx\right|^2} = \frac{h\pi^2 \omega \mu_0 \mu_\perp}{4a\beta_{10}} \quad (5)$$

where E_z and H_x are given in (1). By employing periodic analysis of microwave networks [18] for the unit cell of Fig. 4(b), the dispersion relation of the overall structure is calculated as

$$\cos(\gamma l_{\text{cell}}) = \cos(\beta_{10} l_{\text{cell}}) + \frac{j}{2}\frac{Z_{10}}{Z_p}\sin(\beta_{10} l_{\text{cell}}) \quad (6)$$

where Z_p is given in (3) and $\gamma = \beta + j\alpha$ is the propagation constant of the CSRR-loaded waveguide.

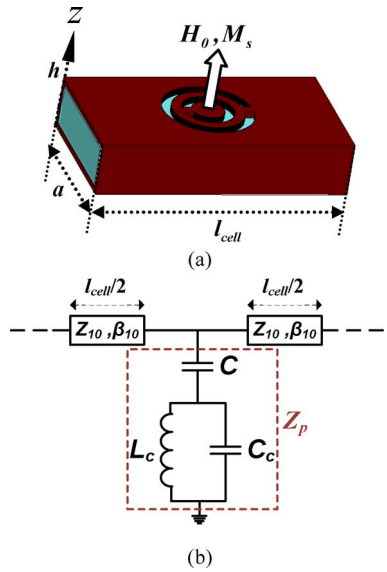

Fig. 4. (a) Ferrite rectangular waveguide loaded with the unit cell of CSRR. (b) Equivalent circuit model of ferrite rectangular waveguide loaded with the unit cell of CSRR.

Fig. 5 shows the dispersion diagram obtained from (6) for a 4 mm-wide and 0.5 mm-high waveguide filled with yttrium iron garnet (YIG) ferrite material subject to a dc bias magnetic field of 400 Oe. The diagram clearly contains a region where the phase velocity ω/β and the group velocity $d\omega/d\beta$ have opposite signs. This region is located between the frequency ω_s ($\omega_s/2\pi = 5.20$ GHz), i.e., the frequency where Z_p of the CSRR starts to show inductive characteristics, and $\omega_H + \omega_M$ ($(\omega_H + \omega_M)/2\pi = 6$ GHz) at which the effective permeability ceases to be negative. The negative effective permittivity caused by the CSRRs coincides with the negative sign of the (real part of) $\mu_\perp$ and yields the left-handed properties observed. Beyond $\omega_H + \omega_M$, the permeability becomes positive, while the negative permittivity persists until ω_0 ($\omega_0/2\pi = 10$ GHz). Thus, in between $\omega_H + \omega_M$ and ω_0, no propagation takes place, which is manifested in Fig. 5 by a zero real part and large imaginary part of the propagation constant $\gamma = \beta + j\alpha$. The same situation exists for $\omega_\perp < \omega < \omega_s$, ($\omega_\perp/2\pi = 2.6$ GHz), but now due to a negative permeability and a positive permittivity. Above ω_0, both effective permittivity and permeability of the structure become positive so that normal, right-handed propagation is expected (see the region above 10 GHz in Fig. 5). The cutoff frequency of this normal wave will depend on the waveguide width as in case of an ordinary waveguide.

III. Full-Wave Simulations

To verify the theoretical result of Section II, the proposed structure of Fig. 1 is simulated by commercial software HFSS that utilized an FEM. In all simulations, YIG was used with the same properties as listed in the caption of Fig. 5. The simulated transmission characteristics of the device is shown in Fig. 6. To have a better comparison, the simulation results of a ferrite-filled rectangular waveguide without CSRRs are also shown. The simulations exhibit LH response from 5.21 to 6.03 GHz, where the analytical LH response is in the frequency range between 5.20 and 6 GHz (see Fig. 5). This confirms the validity of equivalent

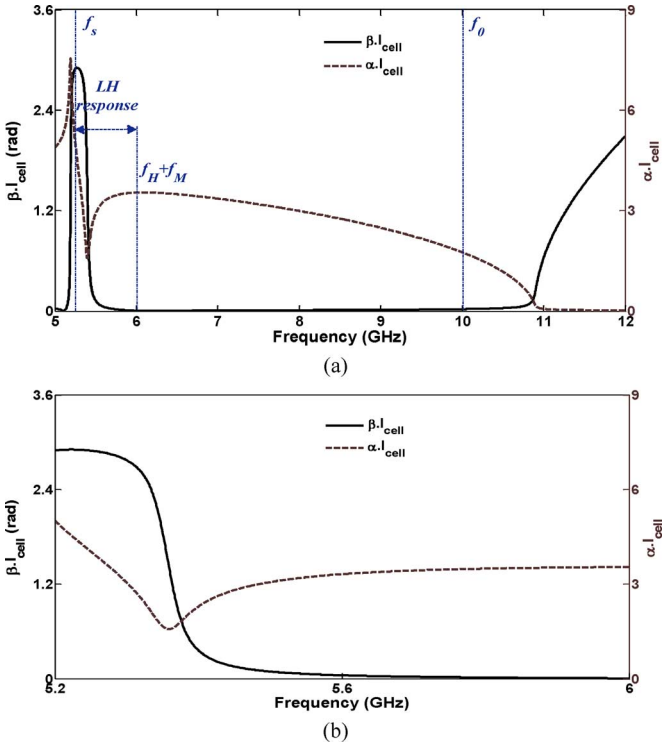

Fig. 5. Dispersion diagram calculated by (6). (a) Frequency range from 5 to 12 GHz. (b) Magnification of the LH range from 5.20 to 6 GHz. $h = 0.5$ mm, $a = 4$ mm, $l_{\rm cell} = 4.5$ mm, $H_0 = 400$ Oe, $M_s = 0.173$ T, $\varepsilon = 15.3$, $\alpha = 0.007$, $C_c = 1.54$ pF, $C = 0.54$ pF, $L_c = 2(\mu)^{1/2}/(1+(\mu)^{1/2}) \times 0.48$ nH.

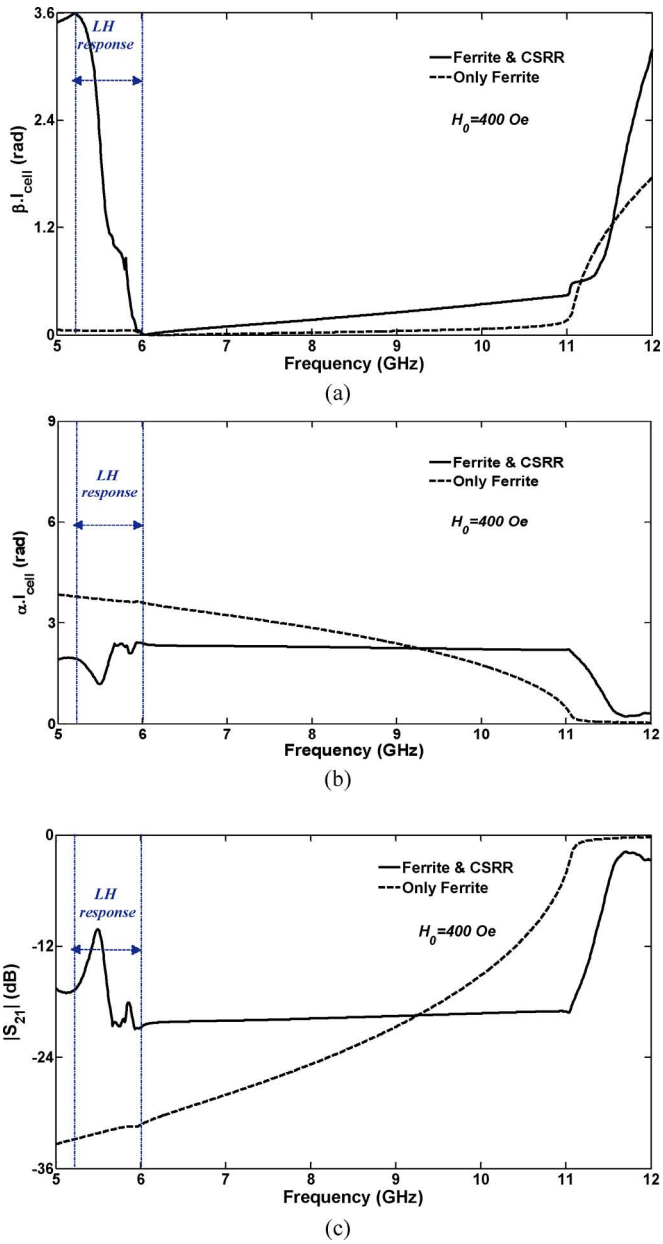

Fig. 6. Full-wave simulation results for the transmission characteristics of a ferrite-filled waveguide with and without CSRRs. (a) Phase shift per unit cell, $\beta \cdot l_{\rm cell}$. (b) Leakage factor per unit cell, $\alpha \cdot l_{\rm cell}$. (c) Transmission coefficient per unit cell. $h = 0.5$ mm, $a = 4$ mm, $l_{\rm cell} = 4.5$ mm, the number of cells $\mathrm{N} = 20$. CSRR dimensions are $r_{\rm out} = 1.5$ mm and $d = c = 0.3$ mm. The full-wave β is obtained by phase unwrapping and shifting (i.e., $\beta = |-\mathrm{unwrapped-phase}(\mathrm{S}_{21})/(\mathrm{N}\, l_{\rm cell}) + 2\pi m|$, where m is an integer corresponding to the frequency where the guided wavelength is infinite, [6]), and full-wave α is obtained by $\alpha = -\ln|\mathrm{S}_{21}|/(\mathrm{N}\, l_{\rm cell})$.

circuit model given in Fig. 4. In the absence of CSRRs, the LH band disappears due to the negative permeability and positive permittivity of ferrite layer (see Fig. 6). As shown in Fig. 6(c), in the LH band, the insertion loss is high due to magnetic loss of ferrite layer. The loss problem is under studies; it may be developed by using single crystal of yttrium iron garnet [10].

The main advantage of a ferrite-based LH line is the magnetic bias tunability. Based on theoretical results given in Section II, the LH response of the proposed structure is in frequency range between ω_s and $\omega_H + \omega_M$. As shown in Table I, by varying the magnetic bias field H_0, both the upper and lower limits can be tuned. Tunability of the upper limit $(\omega_H + \omega_M)$ is easily understood given the definition of ω_H. The lower frequency limit ω_s depends on (4), which is a function of μ that, in turn, depends on H_0. Fig. 7 shows the tunability of LH region for the proposed structure in Fig. 1. As shown in this figure, increasing H_0 will lead to a shift in LH response to higher frequencies.

IV. Conclusion

In this paper, a tunable, ferrite-based left-handed waveguide has been proposed. The main idea behind this structure is to achieve left-handed behavior by the combination of the negative permeability of the ferrite material and negative permittivity of the CSRR array. The idea has been verified by equivalent circuit and numerical analysis. In contrast to previous works, the proposed CRLH structure is easy to design and fabricate and does not require any discrete chip components and vias. It is, as such, a good candidate for design of microwave devices with tunable metamaterial behavior.

Appendix

Consider an infinitely thin current sheet carrying the surface current $\boldsymbol{J}_s = \boldsymbol{J}_{s,x}\hat{\boldsymbol{x}} + \boldsymbol{J}_{s,y}\hat{\boldsymbol{y}}$ on top of an infinitely thick ferrite substrate that is magnetized normal to its surface (z-direction). In the quasi-static approximation, the magnetic field may be written as

$$\boldsymbol{H}^{\pm} = \nabla\psi^{\pm} \tag{7}$$

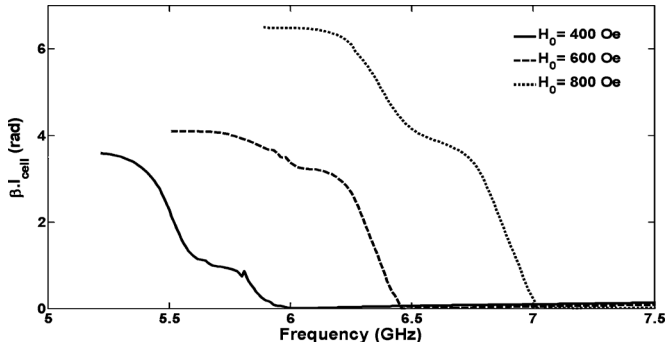

Fig. 7. Simulated phase shift per unit cell for the proposed LH structure under different magnetic bias fields.

TABLE I
TUNABILITY OF UPPER AND LOWER LIMIT OF LH BAND

Magnetic Bias Field (Oe)	Lower Limit (GHz)		Upper Limit (GHz)	
	Theoretical	Simulated	Theoretical	Simulated
400	5.20	5.21	6.00	6.03
600	5.30	5.50	6.52	6.59
800	5.44	5.88	7.08	7.18

with ψ^+, ψ^- the magnetic potential above $(z > 0)$ and below $(z < 0)$ the current sheet, respectively. These potentials satisfy the Walker equations [13]

$$\left(\frac{\partial^2}{\partial x^2} + \frac{\partial^2}{\partial y^2} + \frac{\partial^2}{\partial z^2}\right)\psi^+ = 0 \tag{8}$$

and

$$\left(\frac{\partial^2}{\partial x^2} + \frac{\partial^2}{\partial y^2} + \frac{1}{\mu}\frac{\partial^2}{\partial z^2}\right)\psi^- = 0. \tag{9}$$

As one crosses the current sheet at $z = 0$

$$B_z = \mu_0 \frac{\partial \psi^{\pm}}{\partial z} \tag{10}$$

must remain continuous, while the tangential component of the magnetic field must satisfy

$$\boldsymbol{H}^+(x, y, 0) - \boldsymbol{H}^-(x, y, 0) = \boldsymbol{J}_s(x, y) \times \hat{\boldsymbol{z}}. \tag{11}$$

We apply spatial Fourier transforms in x- and y-directions to both (8) and (9), solve the resulting differential equations, match the solutions using (10) and (11), and take the inverse Fourier transform back to the x, y domain. The result for the normal component of the magnetic flux density is

$$B_z = \frac{\partial A_y}{\partial x} - \frac{\partial A_x}{\partial y} \tag{12}$$

where A_x, A_y are the tangential components of the vector potential which at $z = 0$ are given by

$$A_x(x, y, 0) = \frac{\mu_0 \mu_{\text{eff}}}{4\pi} \int_s \frac{J_x(x', y')}{R} dx' dy' \tag{13}$$

$$A_y(x, y, 0) = \frac{\mu_0 \mu_{\text{eff}}}{4\pi} \int_s \frac{J_y(x', y')}{R} dx' dy' \tag{14}$$

$$R = \sqrt{(x - x')^2 + (y - y')^2} \tag{15}$$

with μ_{eff} given by (4). These expressions may be used to calculate the inductance of any current-carrying structure at $z = 0$ like the metals comprising a CSRR. However, note that the difference between such a calculation and one where the substrate is nonmagnetic is just due to the constant μ_{eff}. Therefore, if the inductance on a nonmagnetic substrate is known, it may be multiplied by μ_{eff} to yield the result on an infinitely thick, normally magnetized ferrite layer.

REFERENCES

[1] D. R. Smith, W. J. Padilla, D. C. Vier, S. C. Nemat-Nasser, and S. Schultz, "Composite medium with simultaneously negative permeability and permittivity," *Phys. Rev. Lett.*, vol. 84, no. 18, pp. 4184–4187, May 2000.

[2] C. Caloz and T. Itoh, "Transmission line approach of left-handed (LH) structures and microstrip realization of a low-loss broadband LH filter," *IEEE Trans. Antennas Propag.*, vol. 52, no. 5, pp. 1159–1166, May 2004.

[3] T. Hand and S. Cummer, "Characterization of tunable metamaterial elements using MEMS switches," *IEEE Antennas Wireless Propag. Lett.*, vol. 6, pp. 401–404, 2007.

[4] T. Hand and S. Cummer, "Frequency tunable electromagnetic metamaterial using ferroelectric loaded split rings," *J. Appl. Phys.*, vol. 6, pp. 066105–066105/3, Mar. 2008.

[5] G. Dewar, "The applicability of ferrimagnetic hosts to nanostructured negative index of refraction (left-handed) materials," in *Proc. SPIE*, 2002, vol. 4806, pp. 156–166.

[6] T. Kodera and C. Caloz, "Uniform ferrite loaded open waveguide structure with CRLH response and it's application to a novel backfire-to-endfire leaky wave antenna," *IEEE Trans. Microw. Theory Tech.*, vol. 57, no. 4, pp. 784–795, Apr. 2009.

[7] T. Kodera and C. Caloz, "Integrated leaky wave antenna-duplexer/diplexer using CRLH uniform ferrite-loaded open waveguide," *IEEE Trans. Antennas Propag.*, vol. 58, no. 8, pp. 2508–2514, Aug. 2010.

[8] M. Abdalla and Z. Hu, "Nonreciprocal left handed coplanar waveguide over ferrite substrate with only shunt inductive load," *Microw. Opt. Technol. Lett.*, vol. 49, pp. 2810–2814, Nov. 2007.

[9] M. Abdalla and Z. Hu, "Design and analysis of tunable left handed zeroth-order resonator on ferrite substrate," *IEEE Trans. Magn.*, vol. 44, no. 11, pp. 3095–3098, Nov. 2008.

[10] M. Tsutsumi and K. Okubo, "Left-handed characterization of ferrite microstrip line magnetized to wave propagation," *IEEE Trans. Magn.*, vol. 45, no. 10, pp. 4207–4210, Oct. 2009.

[11] K. Okubo and M. Tsutsumi, "Effect of nonuniform magnetic field on left handed ferrite microstrip line," in *Proc. APMC*, 2006, pp. 1769–1772.

[12] B. Lax and K. J. Button, "Theory of ferrites in rectangular waveguides," *IRE Trans. Antennas Propag.*, vol. AP-4, no. 3, pp. 531–537, Jul. 1956.

[13] A. G. Gurevich and G. A. Melkov, *Magnetization Oscillations and Waves*. Boca Raton, FL, USA: CRC, 1996, pp. 123–125.

[14] J. D. Baena, J. Bonache, F. Martin, R. Marqués, F. Falcone, T. Lopetegi, M. A. G. Laso, J. Garcia, I. Gil, and M. Sorolla, "Equivalent circuit models for split ring resonators and complementary split rings resonators coupled to planar transmission lines," *IEEE Trans. Microw. Theory Tech.*, vol. 53, no. 4, pp. 1451–1461, Apr. 2005.

[15] F. Falcone, T. Lopetegi, J. D. Baena, R. Marqués, F. Martin, and M. Sorolla, "Effective negative-ε stopband microstrip lines based on complementary split ring resonators," *IEEE Microw. Wireless Compon. Lett.*, vol. 14, no. 6, pp. 280–282, Jun. 2004.

[16] F. Aznar, M. Gill, J. Bonache, L. Jelinek, J. D. Baena, R. Marqués, and F. Martin, "Characterization of miniaturized metamaterial resonators coupled to planar transmission line through parameter extraction," *J. Appl. Phys.*, vol. 104, pp. 114501–114501/7, Dec. 2008.

[17] C. A. Balanis, *Advanced Engineering Electromagnetics*. New York, NY, USA: Wiley, 1989.

[18] R. E. Collin, *Foundations for Microwave Engineering*, 2nd ed. New York, NY, USA: McGraw-Hill, 1992, pp. 552–570.